JACS
JOURNAL OF THE AMERICAN CHEMICAL SOCIETY
Article
pubs.acs.org/JACS

Reactivity of Hydride Bridges in High-Spin [3M−3(μ-H)] Clusters (M = Fe^{II}, Co^{II})

Yousoon Lee,[†] Kevin J. Anderton,[†] Forrest T. Sloane,[†] David M. Ermert,[†] Khalil A. Abboud,[†] Ricardo García-Serres,[‡] and Leslie J. Murray*[,†]

[†]Center for Catalysis and Department of Chemistry, University of Florida, Gainesville, Florida 32611, United States
[‡]Université Grenoble Alpes, LCBM/PMB and CEA, iRTSV/CBM/PMB and CNRS, UMR 5249, LCBM/PMB, 38000 Grenoble, France

Supporting Information

ABSTRACT: The designed [3M−3(μ-H)] clusters (M = Fe^{II}, Co^{II}) Fe_3H_3L (**1-H**) and Co_3H_3L (**2-H**) [where L^{3-} is a tris(β-diketiminate) cyclophane] were synthesized by treating the corresponding M_3Br_3L complexes with $KBEt_3H$. From single-crystal X-ray analysis, the hydride ligands are sterically protected by the cyclophane ligand, and these complexes selectively react with CO_2 over other unsaturated substrates (e.g., CS_2, Me_3SiCCH, C_2H_2, and CH_3CN). The reaction of **1-H** or **2-H** with CO_2 at room temperature yielded $Fe_3(OCHO)(H)_2L$ (**1-CO$_2$**) or $Co_3(OCHO)(H)_2L$ (**2-CO$_2$**), respectively, which evidence the differential reactivity of the hydride ligands within these complexes. The analogous reactions at elevated temperatures revealed a distinct difference in the reactivity pattern for **2-H** as compared to **1-H**; $Fe_3(OCHO)_3L$ (**1-3CO$_2$**) was generated from **1-H**, while **2-H** afforded only **2-CO$_2$**.

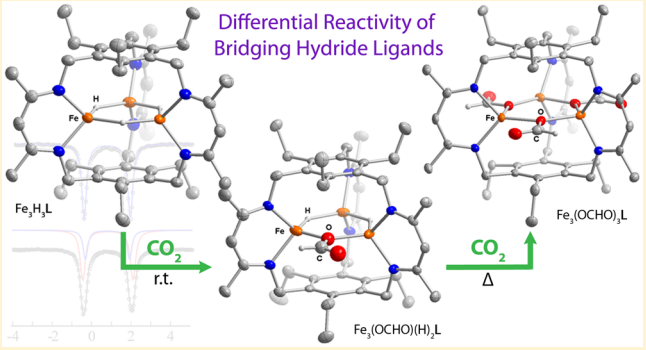

CO_2 is a potential source for more reactive C1 compounds (e.g., carbon monoxide, methanol, methane, or formate) that can either be used directly as fuels (e.g., formate in fuel cells) or as a feedstock for the synthesis of higher molecular weight hydrocarbons (e.g., CO in Fischer−Tropsch synthesis).[1] Transition-metal hydrides, generated either electrochemically or through reaction with a sacrificial hydride source or dihydrogen, have attracted considerable attention as a means to utilize carbon dioxide. Normal hydride insertion into CO_2, in which the nucleophilic hydride attacks the π* orbital on the C atom in carbon dioxide to generate formate, is the predominant mechanism for substrate reduction by M−H groups.[1a,2] The hydride donor ability or the hydricity of the metal−hydride is defined as the energy of heterolytic dissociation of $[LM-H]^{n+}$ into $[LM]^{(n+1)+}$ and H^-. The hydricity of a hydride donor must be less than ∼44 kcal/mol in order to react with carbon dioxide.[3] More importantly, hydricity correlates with selectivity for CO_2 over other substrates and can be used in conjunction with other thermodynamic parameters (e.g., pK_a of the related metal−dihydride complex) to design catalytic systems.[4] Hydricity and the rate of H^- transfer are governed primarily by electronic effects.[5] For example, *trans*-$Cp(CO)_2(PPh_3)MoH$ reacts ∼1500-fold faster than $Cp(CO)_3MoH$ with Ph_3C^+, but *trans*-$Cp(CO)_2(PCy_3)MoH$ reacts only 10 times slower than *trans*-$Cp(CO)_2(PMe_3)MoH$ with the same hydride acceptor.[6]

The spin state of the complex or cluster and the coordination mode of the hydride can be used to tune the reactivity. First, hydride ligands in high-spin metal complexes are typically more hydridic than those in low-spin complexes.[6a,7] Second, terminal hydrides are more reactive than the corresponding bridging hydrides. Terminal hydrides in hydrogenase model compounds reported by Rauchfuss et al. are more reactive toward protonation,[8] and isotopic labeling studies indicate that the bridging hydride in $(\mu\text{-H})Fe_2(pdt)(CO)_2(dppv)_2$ [pdt =1,3-propanedithiolate, dppv = *cis*-1,2-$C_2H_2(PPh_2)_2$] is a spectator during proton reduction.[9] More broadly, bridging hydrides are commonly invoked intermediates in biological systems and function to store reducing equivalents and/or to limit adventitious side reactions (e.g., protonation). For example, μ-hydrides are proposed in mechanisms for the reduction of dinitrogen to ammonia at the iron−molybdenum cofactor (FeMoco) of nitrogenases.[10] ^{1,2}H ENDOR data suggest that the E_4 state of FeMoco contains two μ_2-hydride ligands, which may migrate to one Fe center and reductively eliminate to generate a transient low-valent iron ion (Scheme 1A).[10a,b,11] Similar fluxional coordination of hydride donors between bridging and terminal modes has been observed in a number of hydride-decorated metal clusters supported by strong-field ligands, such as $H(\mu\text{-H})Os(CO)_3$, $H_4Ru_4(CO)_{12-x}(P(OCH_3)_3)_x$, and $(OC)_3HFe(\mu\text{-PCy}_2)Pt(PEt_3)_2$.[12] However, high-spin multinuclear transition-metal hydrides that mirror

Received: May 19, 2015
Published: August 13, 2015

DOI: 10.1021/jacs.5b05204
J. Am. Chem. Soc. 2015, 137, 10610−10617

Scheme 1

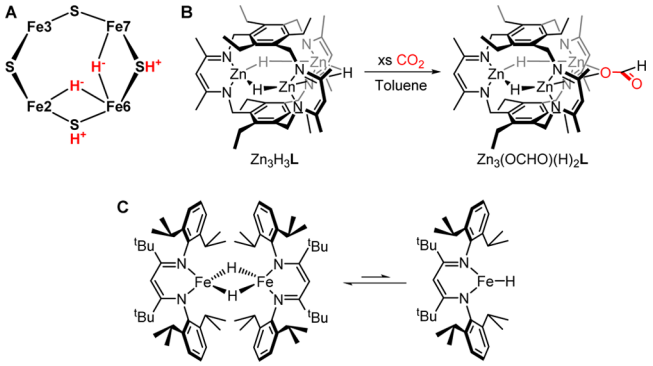

the reduced state of FeMoco remain uncommon, and moreover, the precedents are limited to self-assembled dimeric clusters.[7,13]

In our previous work with a trizinc trihydride complex, Zn_3H_3L [where L^{3-} is a tris(β-diketiminate) cyclophane], we found that the reactivity of the hydride ligands was dramatically dampened as compared to monometallic complexes or binary zinc hydride (Scheme 1B).[14] The narrow substrate specificity exhibited by Zn_3H_3L contrasts with the broad substrate scope for hydride insertion by mono- or dinuclear (β-diketiminato)−iron(II) (Scheme 1C) and −zinc(II) hydrides.[7a,c,15] In addition, the self-assembled diiron(II) hydrides also undergo reductive elimination of H_2 to generate iron(I) species, which coordinate or activate N_2.[7a,d] We therefore targeted trimetallic trihyride complexes of late 3d metals supported by our cyclophane ligand, with specific interest in unmasking low-valent metal centers and examining the effect, if any, of metal ion on the substrate specificity for hydride transfer. Here, we report the synthesis and reactivity of two [3M−3(μ_2-H)] clusters (M = Fe^{II}, Co^{II}) supported by a tris(β-diketiminate) cyclophane. These complexes react with CO_2 but are unreactive toward other unsaturated substrates (e.g., CS_2, Me_3SiCCH, C_2H_2, and CH_3CN). In both complexes, the three hydride donors have different reactivities (i.e., the first is significantly more reactive than the other two), which allows access to trimetallic clusters bearing two hydride donors. The reactivity of the two remaining hydrides with CO_2 is also metal ion dependent, which suggests that M−H bond strength and possibly access to terminal or asymmetric bridging modes can be used to control reactivity and specificity.

EXPERIMENTAL METHODS

General Considerations. Unless specified otherwise, all operations were performed under a dry, air-free atmosphere using a dinitrogen-filled MBraun Unilab glovebox or standard Schlenk techniques. ^{1}H NMR spectra were recorded on a Varian Unity Inova 500 MHz spectrometer. Chemical shifts were referenced to solvent resonances at δ_H = 7.16 ppm for C_6D_6 and at δ_H = 2.08, 6.97, 7.01, and 7.09 ppm for toluene-d_8. Solution magnetic susceptibilities were determined by Evans' method.[16] Infrared spectra were recorded in a nitrogen-filled glovebox as solids on a Bruker Alpha FTIR with an ATR diamond crystal stage using the Opus 7.0 software package. Cyclic voltammetry experiments were performed in an N_2-filled glovebox using a Princeton Applied Research Versastat II potentiostat and a three-electrode setup (1 mm Pt button working electrode, Au coil counter electrode, and $Ag/AgNO_3$ reference electrode) with electrodes purchased from BASi, Inc. and/or CH Instruments, Inc. Complete Analysis Laboratories, Inc. (Parsippany, NJ) conducted elemental analyses on samples prepared and shipped in ampules sealed under vacuum. Tetrahydrofuran (THF), toluene, benzene, pentane, hexanes, and dichloromethane were purified using either a Glass-Contour or Innovative Technologies solvent purification system and stored over 3 Å molecular sieves prior to use. The water content of each solvent was measured using a Mettler Toledo C20 Coulometric Karl Fischer Titrator prior to use and was below 1 ppm in all cases. Celite and 3 Å molecular sieves were dried at 220 °C under vacuum overnight. Anhydrous $FeBr_2$ was purchased from Acros Organics and dried further under an N_2 stream at 220 °C overnight. Anhydrous $CoBr_2$ was prepared from $CoBr_2 \cdot 6H_2O$ by heating in contact with a P_2O_5 trap and then treating with thionyl bromide under reflux conditions, filtering, washing with benzene, and drying under vacuum overnight. $KBEt_3H$ was prepared according to a previous report[17] and recrystallized by layering hexanes onto a toluene solution of the compound. H_3L,[18] Fe_3Br_3L (**1**),[18] and benzylpotassium[19] were prepared according to published procedures. CO_2 (research grade, 99.999%) was purchased from Airgas, Inc. and purified by passage through a Restek O_2 scrubber column and two cold traps (LN_2/$CHCl_3$). $^{13}CO_2$ was purchased from Cambridge Isotope Laboratories and used as received. All other reagents were purchased from Sigma-Aldrich and used without further purification. Details of X-ray crystallographic data collection and structure solutions are provided in the Supporting Information.

Co_3Br_3L (2). H_3L (1.20 g, 1.74 mmol) and benzylpotassium (746 mg, 5.73 mmol) were combined as solids to which THF (48 mL) was added. The resulting dark purple solution was stirred at room temperature for 30 min, and then volatiles were removed under reduced pressure. To the dried residue was added anhydrous $CoBr_2$ (1.25 g, 5.73 mmol) as a solid, followed by toluene (80 mL). The mixture was stirred at room temperature for 3 h and then at 80 °C overnight. The resulting dark purple slurry was allowed to cool and was then filtered through a plug of Celite (previously rinsed with anhydrous toluene). The filtrate was concentrated to ∼45 mL under vacuum and then heated to 80 °C, filtered through a plug of toluene-rinsed Celite, and stored at −35 °C. After 5 days, 665 mg (0.602 mmol) of a dark purple crystalline powder was isolated. An additional 100 mg (0.0905 mmol) of material was obtained by repeating the precipitation procedure, for a combined yield of 40%. Crystals suitable for single-crystal X-ray analysis were obtained from a vapor diffusion of hexanes to a solution of crude product in THF at room temperature. IR: 2949, 1518, 1457, 1431, 1389, 1371, 1326, 1016 cm^{-1}. Anal. found (calcd) for $C_{45}H_{63}N_6Co_3Br_3$: C, 49.02 (48.93); H, 5.82 (5.75); N, 7.58 (7.61).

Fe_3H_3L (1-H). A colorless solution of $KBEt_3H$ (184 mg, 1.40 mmol) in toluene (30 mL) was added dropwise over the course of 5 min to a red slurry of Fe_3Br_3L (472 mg, 0.431 mmol) in toluene (30 mL), which was stirred with a glass stir bar at room temperature. The reaction became clearer with a color change to dark red-orange after ∼1 h. The reaction was allowed to stir overnight and then filtered through a plug of toluene-rinsed Celite. Volatiles were removed under reduced pressure, and slow cooling of a hot (80 °C), saturated benzene solution of the resulting orange-brown powder to room temperature yielded dark red-orange needle crystals (271 mg, 0.316 mmol, 73%) after 2 days. Crystals suitable for single-crystal X-ray analysis were obtained by cooling a toluene solution of the crude product at −39 °C. IR: 2965, 1526, 1459, 1428, 1397, 1374, 1339, 1021, 731 cm^{-1}. μ_{eff} (C_6D_6, 298 K) = 6.3 μ_B. Anal. found (calcd) for $C_{45}H_{66}N_6Fe_3$: C, 62.83 (62.95); H, 7.78 (7.75); N, 9.73 (9.79); Fe, 19.39 (19.51).

Co_3H_3L (2-H). A colorless solution of $KBEt_3H$ (155 mg, 1.21 mmol) in benzene (40 mL) was added dropwise over the course of 5 min to a purple slurry of Co_3Br_3L (393 mg, 0.356 mmol) in benzene (40 mL), which was stirred with a glass stir bar at room temperature. The reaction mixture changed to dark red-orange over 40 min, after which the reaction was filtered through a plug of benzene-rinsed Celite. The filtrate was frozen and lyophilized to yield a brown powder. Slow cooling of a hot, saturated benzene solution of the crude product yielded dark red-orange needle crystals (193 mg, 0.222 mmol, 62%) after 2 days. Crystals suitable for single-crystal X-ray analysis were obtained from a vapor diffusion of hexanes into a toluene solution of

DOI: 10.1021/jacs.5b05204
J. Am. Chem. Soc. 2015, 137, 10610−10617

the compound. IR: 2868, 1531, 1460, 1430, 1396, 1374, 1351, 1306, 1279, 1247, 1013, 771, 740, 682 cm^{-1}. μ_{eff} (toluene-d_8, 298 K) = 4.1 μ_B. Anal. found (calcd) for $C_{45}H_{66}N_6Co_3$: C, 62.27 (62.28); H, 7.73 (7.67); N, 9.64 (9.68); Co, 20.25 (20.37).

$Fe_3(OCHO)(H)_2L$ (1-CO_2). Fe_3H_3L (89.1 mg, 0.104 mmol) was dissolved in THF (18 mL) in a Schlenk flask equipped with a Teflon stir bar. The solution was degassed by the freeze−pump−thaw method, and then the flask was refilled with CO_2. The reaction solution was stirred under a slow flow of CO_2 for 25 min, sealed, and allowed to stir under a static atmosphere of CO_2 at room temperature. After 22 h, all volatiles were removed from the bright orange solution under reduced pressure. The resulting orange powder was transferred to the glovebox, and the desired product was isolated as an orange microcrystalline powder by vapor diffusion of pentane into a THF solution of the crude product at −35 °C (49.7 mg, 0.0551 mmol, 53%). Crystals suitable for single-crystal X-ray analysis were obtained from a vapor diffusion of pentane into a toluene solution of the compound. IR: 2927, 1676 (C═O), 1519, 1456, 1429, 1397, 1374, 1333, 1214 (C−O), 1017, 731 cm^{-1}. μ_{eff} (toluene-d_8, 298 K) = 6.4 μ_B. Anal. found (calcd) for $C_{46}H_{66}N_6O_2Fe_3$: C, 60.99 (61.21); H, 7.44 (7.37); N, 9.18 (9.31).

$Fe_3(OCHO)_3L$ (1-3CO_2). Fe_3H_3L (24.8 mg, 0.0289 mmol) was dissolved in toluene (5 mL) in a storage tube equipped with a Teflon stir bar. The solution was degassed by the freeze−pump−thaw method, and then the flask was refilled with CO_2, and the contents were stirred under a slow flow of CO_2 for 25 min. The flask was then sealed, and the reaction was heated at 60 °C for 2 d, during which the dark red-orange solution turned bright orange and became turbid. After 5 d, all volatiles were removed under reduced pressure. The resulting tan-orange powder was dissolved in minimal dichloromethane and recrystallized by vapor diffusion with pentane to afford the product as orange crystals (15.4 mg, 0.0155 mmol, 54%). IR: 2927, 1642 (C═O), 1516, 1460, 1431, 1397, 1373, 1324, 1215 (C−O), 1016, 732 cm^{-1}. Anal. found (calcd) for $C_{48}H_{66}N_6O_6Fe_3$: C, 57.99 (58.20); H, 6.88 (6.72); N, 8.20 (8.48).

$Co_3(OCHO)(H)_2L$ (2-CO_2). The reaction was carried out as described for 1-CO_2 using Co_3H_3L (99.5 mg, 0.115 mmol) dissolved in toluene (20 mL). During the course of the reaction, the color of the solution changed from dark red-orange to dark red. After 5 d, volatiles were removed under reduced pressure, and the dark red powder was recrystallized by vapor diffusion of pentane into a benzene solution to give the product as dark red crystals (38.3 mg, 0.0420 mmol, 37%) suitable for single-crystal X-ray analysis. IR: 2967, 1685 (C═O), 1529, 1463, 1430, 1396, 1374, 1339, 1215 (C−O), 1014, 733 cm^{-1}. μ_{eff} (C_6D_6, 298 K) = 5.1 μ_B. Anal. found (calcd) for $C_{46}H_{66}N_6O_2Co_3$: C, 60.66 (60.59); H, 7.42 (7.30); N, 9.07 (9.22).

Reaction of Co_3H_3L with $^{13}CO_2$ (2-$^{13}CO_2$). Co_3H_3L (3.0 mg, 3.49 μmol) was dissolved in toluene (0.6 mL) in a J. Young NMR tube (Wilmad). The solution was degassed by the freeze−pump−thaw method, and then the tube was refilled with ∼1 atm of $^{13}CO_2$ and sealed. After 5 d, all volatiles were evaporated, and the residue was redissolved in toluene. An IR spectrum was recorded by drop-casting the solution onto the ATR stage. IR (cm^{-1}): 1643, 1195 (^{13}CO).

Mössbauer Spectroscopy. All the samples were ground, placed in Delrin sample containers, and sealed with screw caps in an N_2-filled glovebox. Mössbauer spectra were measured either on a low-field Mössbauer spectrometer equipped with a closed-cycle SHI-850-5 cryostat from Janis and SHI or an Oxford Instruments Spectromag 4000 cryostat containing an 8T split-pair superconducting magnet. Both spectrometers were operated in constant acceleration mode in transmission geometry. The isomer shifts are referenced against a room temperature metallic iron foil. Analysis of the data was performed using the program WMOSS (WEB Research).

RESULTS AND DISCUSSION

Using a similar synthetic approach as previously reported for Fe_3Br_3L (**1**),[18] the tricobalt(II) congener Co_3Br_3L (**2**) was prepared in reasonable yield (40%) by reaction of the free-base ligand with benzyl potassium followed by addition of 3 equiv of $CoBr_2$. The solid-state structure revealed a comparable arrangement of the M_3Br_3 core, as observed in **1** and Mn_3Br_3L,[18] as anticipated from the steric constraints imposed by the ligand and the size of the bromide donors (Figure 1).

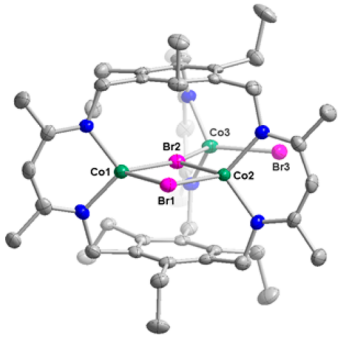

Figure 1. Single-crystal structure of Co_3Br_3L (**2**) at 75% thermal ellipsoid. Hydrogen atoms and a THF solvent molecule have been omitted for clarity. C, N, Co, and Br are depicted as gray, blue, green, and pink ellipsoids, respectively.

Each cobalt center in **2** adopts a pseudotrigonal pyramidal coordination geometry with τ_4 values between 0.87 and 0.89.[20] As for **1**, the ligand is distorted as compared to either the tricopper complexes[21] or the protonated ligand,[18] with a significant dihedral angle [7.5(1)°] between the two arene linkers and a range of distances [0.274(4)−0.576(4) Å] between the metal center and the NCCCN plane of β-diketiminate arm to which it is coordinated.

Treatment of **1** or **2** with 3 equiv of $KBEt_3H$ in toluene or benzene at room temperature afforded the tri(μ-hydrido)-triiron(II) cluster (**1-H**) or tri(μ-hydrido)tricobalt(II) cluster (**2-H**) compounds in good yield (73% and 62%, respectively) (Scheme 2). Previously, the BEt_3 byproduct generated by this

Scheme 2

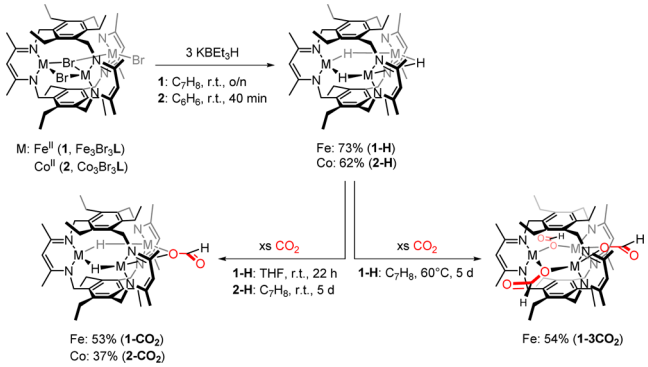

method has been reported to react adventitiously with the iron or cobalt hydride product in the monometallic complexes to afford metal−alkyl species as a side product; we observed no evidence for a similar decomposition reaction in the synthesis of **1-H** or **2-H**.[7a,c] We attribute this difference to the steric protection afforded by our ligand as well as the diminished reactivity of the bridging hydrides in our clusters (vide infra).

From the solid-state structures of **1-H** and **2-H** (Figure 2), the metal ions are held in a pseudotetrahedral coordination environment defined by two hydride donors and two N atoms from a single β-diketiminate arm (τ_4 = 0.89−0.94 for **1-H** and τ_4 = 0.91−0.94 for **2-H**). To our knowledge, **1-H** and **2-H** are

DOI: 10.1021/jacs.5b05204
J. Am. Chem. Soc. 2015, 137, 10610−10617

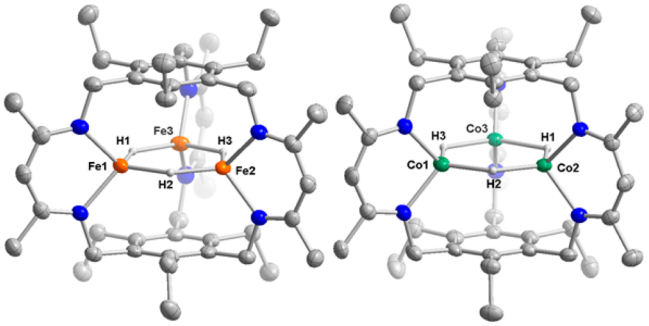

Figure 2. Single-crystal structures of Fe_3H_3L (**1-H**) (left) and Co_3H_3L (**2-H**) (right) at 65% thermal ellipsoid. Solvent molecules, hydrogen atoms except for the hydride ligands, and atoms with minor occupancies have been removed for clarity. C, H, N, Fe, and Co atoms are depicted as gray, light gray, blue, orange, and green ellipsoids or spheres, respectively.

the only late transition-metal clusters that adopt a coplanar $M_3(\mu\text{-H})_3$ motif (M = Fe, Co) and are analogous to the trizinc(II) trihydride complex previously reported by our group.[14] The three μ-H donors were readily located in the Fourier difference map, although some of the hydrides were partially occupied (viz. 92% for one in **1-H**, 99% for all in **2-H**). As expected from the smaller covalent radius of cobalt versus iron, the M−N_L distances (where N_L = β-diketiminate N-donor atom) in **2-H** are shorter [2.014(2)−2.035(3) Å] than those observed for **1-H** [2.039(2)−2.057(2) Å]. The β-diketiminate bite angles have been correlated with the d-electron count of the metal center in monometallic complexes,[22] and a similar trend is observed here with larger bite angles in **2-H** [92.1(1)°−92.5(1)°] than those in **1-H** [90.23(8)°−91.10(8)°]. **1-H** and **2-H** generally feature longer M−N_L bonds and smaller bite angles than self-assembled dimeric (β-diketiminato)metal hydrides [e.g., 1.971(4)−2.022(6) Å for Fe−N_L bonds, 1.961(2)−1.977(2) Å for Co−N_L bonds; 95.0(2)°−95.3(2)° for $\angle N_L$−Fe−N_L, 95.60(6)°−96.02(6)° for $\angle N_L$−Co−N_L].[13a,15a,23] The metal−hydride bond distances [**1-H**, 1.78(3)−1.86(3) Å; **2-H**, 1.83(2)−1.98(2) Å] are significantly longer than previously reported for self-assembled dimers of (β-diketiminato)iron(II)[7a,15a,23,24] and cobalt(II) hydrides[13a] [viz. 1.30(7)−1.69(3) Å for Fe−H, 1.56−1.67 Å for Co−H] and, more broadly, for any other di- or trimetallic complexes of iron [1.51(3)−1.77(3) Å] or cobalt [1.37(8)−1.84(7) Å].[25] The longer than usual M−(μ-H) bond lengths in **1-H** and **2-H** correlate with the longer M−M distances [viz. 3.2570(6)−3.3561(5) Å in **1-H** and 3.3226(7)−3.3473(6) Å in **2-H** vs 2.249(1)−2.8721(4) Å in all the other complexes mentioned above] and more obtuse bond angles observed here.

The structural analysis also revealed that, aside from the major M_3H_3L species, there is/are minor product(s) formed in which two metal atoms with occupancies of 3% for Fe and 2.5% for Co are coordinated in an η^6 fashion to the internal π-face of the benzene caps of the cyclophane ligand (Figures S8 and S9). Previously, we attributed these arene-coordinated metal atoms to low-valent metal ions that shift from the β-diketiminate chelate to the arene upon reduction of **1**.[26] A similar chelate-to-arene shift has been reported for low-valent monometallic β-diketiminate complexes.[27] Considering these (η^6-arene)iron or cobalt centers and the partial occupancies of the hydride ligands, we speculate that either hydride for halide exchange is competitive with reductive elimination of H_2 or that adventitious reduction of the divalent metal ions by $KBEt_3H$ occurs during the syntheses of **1-H** and **2-H**. Holland and co-workers reported reductive elimination of H_2 from a dimeric $Fe_2(\mu\text{-H})_2$ cluster supported by β-diketiminate ligands, which generates an iron(I) species that subsequently reacts with N_2,[7a,d] as well as access to cobalt(I) centers upon reaction of (β-diketiminato)cobalt(II) complexes with $[BEt_3H]^-$.[13b] Given the precedents and the presence of the (η^6-arene)metal centers in the solid-state structures of **1-H** and **2-H**, we attempted to liberate H_2 by broad-wavelength irradiation or prolonged heating at reflux of a toluene solution of either **1-H** or **2-H**. No changes, however, were observed in IR or UV/visible spectra or in the unit cell parameters of the isolated crystalline products after heating or irradiation (i.e., parameters were consistent with **1-H** and **2-H**). Thus, hydride donors in the M_3H_3L family of complexes are not effective masks for low-valent metal centers, at least under the conditions employed.

As reductive elimination of H_2 was not observed for **1-H** and **2-H**, we next set out to test the reaction of these hydride complexes with unsaturated substrates. Similar to the trizinc(II) analog,[14] **1-H** and **2-H** failed to react with carbon disulfide, trimethylsilylacetylene, and acetonitrile and produced an unidentifiable mixture with acetylene. The IR spectra of crude products from these reactions did not indicate the formation of new C−H bonds or weakening of multiple covalent bonds of the substrates, as expected for hydride insertion, or the unit-cell parameters for crystals isolated from the reaction mixtures were comparable to those of **1-H** or **2-H** (data not shown). We subsequently explored the reaction of **1-H** or **2-H** with CO_2 at room temperature and ultimately isolated orange or dark red crystals from the respective reaction mixtures (Scheme 2). The solid-state structures of these two products revealed approximately 1 equiv (based on summed occupancies) of a μ−η^1:η^1-formate ligand disordered over the three possible bridging positions (Figure 3, S10). The products were therefore

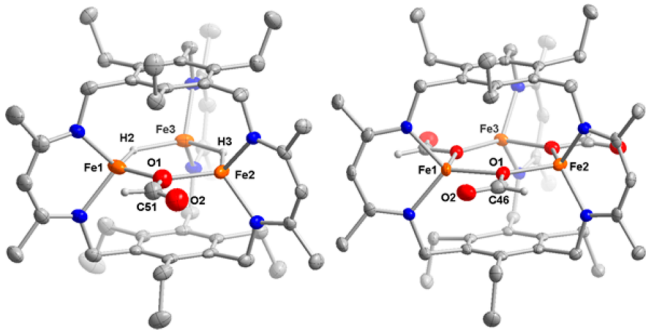

Figure 3. Single-crystal structures of $Fe_3(OCHO)(H)_2L$ (**1-CO_2**) (left) and $Fe_3(OCHO)_3L$ (**1-3CO_2**) (right) at 65% (for **1-CO_2**) or 75% (for **1-3CO_2**) thermal ellipsoid. Solvent molecules, hydrogen atoms except for the hydride and formate ligands, and atoms with minor occupancies have been removed for clarity. The formate ligand (67% occupancy) in **1-CO_2** is co-occupied with 33% H1, and the rest is diffused over the H2 and H3 positions with 25% and 15% occupancies, respectively. C, H, N, O, and Fe atoms are depicted as gray, light gray, blue, red, and orange ellipsoids or spheres, respectively.

formulated as $Fe_3(OCHO)(H)_2L$ (**1-CO_2**) or $Co_3(OCHO)(H)_2L$ (**2-CO_2**), which agrees with combustion analysis data and the product isolated from reaction of Zn_3H_3L with CO_2.[14] Whereas the μ-1,1 coordination mode is common for formate in polynuclear iron complexes,[28] **2-CO_2** represents the first crystallographically characterized example for a discrete cobalt

DOI: 10.1021/jacs.5b05204
J. Am. Chem. Soc. 2015, 137, 10610−10617

cluster, although Co^{II}−(μ-1,1-formate) units have been observed in coordination solids.[29]

The metal−ligand bond distances and angles in **1-CO$_2$** and **2-CO$_2$** are more comparable with those observed in monometallic diketiminate complexes than those for **1-H** and **2-H**.[15a,22] For example, M1 and M2 (M = Fe or Co) bridged by the formate ligand with the highest occupancies (67% for **1-CO$_2$** and 54% for **2-CO$_2$**) have larger N_L−M−N_L or bite angles of 93.25(9)°−94.20(9)° (Fe) and 94.3(1)°−95.0(1)° (Co) than observed in the tri(hydride) precursors. In comparison to models of the active sites of the reduced hemerythrin, ribonucleotide reductase, and methane monooxygenase, the Fe−O bond lengths [1.963(3), 2.041(3) Å] in **1-CO$_2$** are slightly shorter than those values [2.113(2)−2.172(2) Å] and consistent with the lower coordination number in the clusters reported here.[28] Finally, the μ−η^1:η^1-formate moiety possesses localized C═O and C−O bond character based on the bond metrics and is corroborated by the infrared spectra of **1-CO$_2$** or **2-CO$_2$**. We observe C═O stretching modes at 1676 or 1685 cm^{-1} and the C−O stretch at 1214 or 1215 cm^{-1} for **1-CO$_2$** and **2-CO$_2$**, respectively. These absorptions are shifted to 1643 and 1195 cm^{-1} in the product from the reaction of **2-H** with $^{13}CO_2$, which is in good agreement with the calculated values based on the difference in the reduced masses.

Mössbauer spectra and cyclic voltammograms were collected on crystalline samples of **1-H** and **1-CO$_2$** to support the assignment of the triiron product as a monoformate di(hydride) species and to evaluate the redox properties of the trihydride and (formate)di(hydride) complexes. The Mössbauer spectrum of **1-H** acquired at 80 K and under zero-applied field consists of one symmetric quadrupole doublet with an isomer shift, δ, of 0.79 mm/s and a quadrupole splitting, ΔE_Q, of 2.34 mm/s (Figure 4A and Table S1). These values are

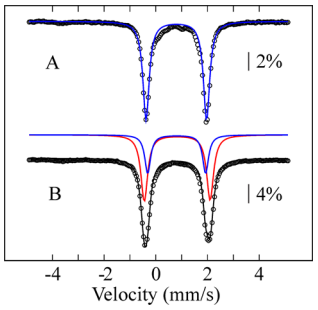

Figure 4. Mössbauer spectra (80 K) of (A) **1-H** and (B) **1-CO$_2$**. The circles represent the experimental data points. The colored lines are simulated quadrupole doublets, as described in the text (see Table S1 for simulation parameters), whereas the black, solid line is a composite spectrum obtained by combining individual doublets.

expected for a high-spin ferrous site in a tetrahedral coordination environment,[30] and the symmetric, narrow doublet agrees with the solid-state structure (i.e., the electric field gradient around each iron center is approximately equivalent). A minor proportion of the absorption (~5%, not plotted) is ascribed to ferrous and ferric impurities. Mössbauer spectra of **1-H** recorded at 4.2 K in applied magnetic fields agree with the model of three ferrous centers antiferromagnetically coupled to an S = 0 ground state (Figure 5). Simulation of the data with an S = 0 Hamiltonian did not yield a good fit, presumably owing to the presence of a thermally accessible excited (S = 1) state (Figure 5, red solid line). In the equilateral

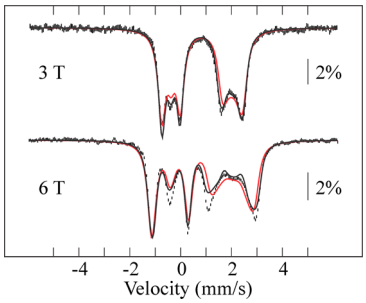

Figure 5. Powder 4.2 K Mössbauer spectra of **1-H**, in a magnetic field of 3 or 6 T applied parallel to the direction of the γ-beam. The vertical bars represent experimental points. Red, solid lines correspond to the best theoretical fit assuming a diamagnetic (S = 0) ground state. Black, solid lines correspond to a theoretical simulation assuming one single site with $S = {}^1/_2$ exchange-coupled to an $S' = {}^1/_2$ spin with the Hamiltonian $\boldsymbol{H} = \boldsymbol{J}'\mathbf{S}\cdot\mathbf{S}' + g_0\beta\mathbf{B}\cdot(\mathbf{S}+\mathbf{S}') + H_{hf}$, the last term being the usual hyperfine spin Hamiltonian. The best fit was obtained with J' = 11.3 cm^{-1} and the parameters are listed in Table S2.

triangle approximation ($\boldsymbol{H} = J\,[\mathbf{S_1}\cdot\mathbf{S_2} + \mathbf{S_2}\cdot\mathbf{S_3} + \mathbf{S_3}\cdot\mathbf{S_1}]$), which is fairly reasonable given the near-perfect D_{3h} symmetry of the crystal structure, the lowest excited multiplets are three degenerate triplets. In order to introduce an excited S = 1 state in the simulation, we assumed a fictitious $S = {}^1/_2$ spin antiferromagnetically coupled to a second $S' = {}^1/_2$ spin. The simulation was performed in the fast relaxation limit. The resulting fit was significantly improved with respect to the diamagnetic approximation (Figure 5, black solid lines, and Table S2), although this simple model neglects asymmetry and ZFS parameters. The fit yielded an energy gap of 11.3 cm^{-1} between the ground singlet and the excited triplet. Taking into account degeneracy and without considering higher energy multiplets, this translates into a coupling constant of J = 14.5 cm^{-1} between ferrous centers. This value should be taken as a coarse estimate, but its magnitude corresponds to what is expected for a hydride bridge.[7a,31]

The spectrum of **1-CO$_2$** resembles that of **1-H** but exhibits a broader, slightly asymmetric doublet (Figure 4B). The data could not be satisfactorily simulated with a single (even asymmetric) quadrupole doublet. Instead, applying two symmetric doublets in a ~ 1:2 ratio improved the fit significantly (Table S1). This result corroborates the expected structure, in which only one iron atom has the same coordination as in **1-H** and the other two are in similar environments (i.e., one hydride and one formate O atom). In the cyclic voltammograms of **1-** and **2-H** in dimethoxyethane, a reversible reductive wave is observed for both **1-** and **2-H** at comparable potential, with **2-H** at ~30 mV lower potential (viz. $E_{1/2}$ = −2.65 V for **1-H** vs $E_{1/2}$ = −2.68 V for **2-H**, referenced to Fc/Fc^+, Figures S11 and S12). However, redox couples were observed for **1-**/**2-CO$_2$** at the potentials within error for the respective hydride complexes (Figures S13 and S14).

We subsequently sought to evaluate whether the two remaining hydrides could react with CO_2 under slightly harsher conditions. Although the synthesis of **2-CO$_2$** was reproducible in toluene at ambient temperature, **1-H** first afforded **1-CO$_2$** and then evolved into a complex mixture of products, as suggested by multiple C═O stretches in the IR spectra (data not shown), whereas the reaction in THF reproducibly yielded **1-CO$_2$**. The appearance of multiple absorptions with energies consistent with C═O vibrations suggested that additional products are formed possibly from reaction of the remaining

DOI: 10.1021/jacs.5b05204
J. Am. Chem. Soc. 2015, 137, 10610−10617

hydrides with excess CO_2. Reaction of **1-H** with CO_2 in toluene at 60 °C afforded the triformate species, $Fe_3(OCHO)_3L$ (**1-3CO$_2$**), which was isolated in a good crystalline yield (54%). In the IR spectra of **1-3CO$_2$**, we observed C═O and C−O vibrations at 1642 and 1215 cm^{-1}, respectively. Each formate in **1-3CO$_2$** coordinates to the iron centers in a μ−η^1:η^1-fashion with an additional weak interaction between the dangling O atom of each formate ligand and the closest Fe atom (Figure 3). Consequently, the Fe−μ-O bond lengths alternate between longer and shorter distances, with the shorter values corresponding to the presence of an interaction with a dangling O atom. In addition, there is also a slight rotation about the C−N bond that connects each β-diketiminate arm to the benzene linkers. This rotation, which may arise from the steric constraints of accommodating a formate donor in each μ_2 site, gears the ligand into a C_{3h} conformation rather than a pseudo-D_{3h} one. There is also a contraction in the Fe−N_L bond distances in **1-3CO$_2$** [1.984(2)−1.992(2) Å] as compared to either **1-H** or **1-CO$_2$** and concomitant increases in the N_L−Fe−N_L bond angles [98.62(6)°−99.57(6)°] to values significantly closer to those for mononuclear diketiminatoiron(II) complexes.[22] In contrast to **1-H**, heating the reaction of **2-H** with CO_2 up to 80 °C did not alter the speciation of the products and resulted in isolation of only **2-CO$_2$** and no evidence for further incorporation of CO_2.

The substrate specificity, the differential reactivity of the hydride ligands in **1-H** and **2-H**, and the selective synthesis of **1-** and **2-CO$_2$** and **1-3CO$_2$** are atypical of high-spin 3d metal hydrides.[7b] We recently communicated similar specificity for the trizinc(II) analog of **1-H**, which reacts only with carbon dioxide and not varied protic (e.g., water) and unsaturated substrates (e.g., acetonitrile) based on IR and NMR spectra.[14] It appears generally then that the hydride donor strength of trimetallic trihydride complexes of our ligand is tuned narrowly to be highly specific for CO_2. We estimate the hydricity of the first hydride to react in **1-H** and **2-H** to lie within the range of BEt_3 and CO_2, which are 26 and 44 kcal/mol (values reported for acetonitrile solutions), respectively.[32] The lower limit is based on the synthetic protocol in which **1-H** and **2-H** are isolated in the presence of BEt_3. Upon incorporation of one formate to afford **1-CO$_2$** and **2-CO$_2$**, however, the hydricity of the remaining two hydrides is comparable to or exceeds that of CO_2, either because additional thermal energy is required for hydride transfer (Fe) or because these ligands are unreactive (Co). Our estimation of **1-H** and **2-H** does not account for the free energy associated with formate coordination to the respective clusters, which can be significant. Recently, Fong and Peters suggested that the strength of the metal−formate interaction provides the necessary energy to drive hydride transfer to CO_2 because this reaction was predicted to be uphill if only the hydricity of the Fe−H species and formate is considered.[33] Similarly, iron-hydrides present in the reduced state of FeMoco in a reengineered enzyme are speculated to facilitate the initial step of the reduction of CO_2 to form an iron-bound formate intermediate, and the coordination of the formate is considered integral to that mechanism.[34] Our analysis also excludes any kinetic contributions to reactivity; that is, the reaction with substrates other than CO_2 may be thermodynamically favored, but kinetically disfavored. Although steric effects typically contribute less to the hydride transfer rate than electronic effects do, those studies examined the effect of substituents on phosphine donors in piano stool cyclopentadienyl complexes.[6a] The unusual steric constraints imposed by this cyclophane ligand, L^{3-}, such as the close flanking of the hydride by two ethyl substituents, may have a more pronounced effect on the kinetics of hydride transfer than the size of the alkyl substituent on the phosphine donor in the piano stool compounds.

We envision two possible mechanisms for hydride transfer from **1-H** and **2-H** to CO_2 (Scheme 3). For mechanism A, direct insertion of the bridging hydride into carbon dioxide and subsequent rearrangement would afford the observed monoformate products. Each hydride insertion requires cleavage of two M−H bonds, and these bond strengths change as a function of formate incorporation (i.e., after the first CO_2 insertion), which ultimately diminishes reactivity. The reactivity of only one hydride in polyhydride complexes with carbon dioxide has also previously been demonstrated.[35] M−H bond strength is expected to be greater for Co than for Fe, which is consistent with the successful synthesis of **1-3CO$_2$** and not the analogous tricobalt species under comparable conditions. Thus, the reactivity of the hydride donors is controlled by virtue of the bridging arrangement of the hydrides as imposed by the ligand (which dampens reactivity) and by the electronic changes upon forming the formate complexes. Bridging hydrides are well-known to be less reactive than terminal ones, as noted above.

Scheme 3

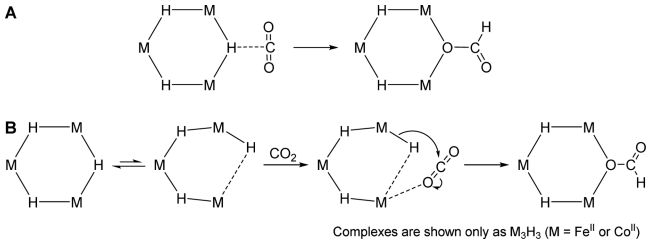

Previously, Holland and co-workers reported that a β-diketiminatoiron(II) hydride is in equilibrium in solution with the di(μ-hydride)diiron complex, but that only the monomer reacts with substrates.[7a,15a] The analogous cobalt compound exists exclusively in the dimeric form and is unreactive toward the substrates tested (e.g., CO_2).[13a] This result also correlates with the decrease in hydricity with increasing the electronegativity of the metal center, which has been reported for metal carbonyl hydride complexes.[5b] Given that we use similar diketiminate donors as in Holland's complexes, we reason that comparable reactivity is plausible for **1-H** and **2-H**. In mechanism B (Scheme 3), the hydride ligands are fluxional and access terminal or asymmetric bridging modes, which allow the hydride to readily insert into CO_2. The partial opening of the hydride bridge would mirror the dimer−monomer equilibrium proposed for the monometallic diketiminate compounds.[7a,15a] Insertion of one molecule of CO_2 may be possible in **1-H** and **2-H** because the cluster is sufficiently flexible to distort (as suggested by the smaller bite angles and longer M−H bond lengths relative to other iron and cobalt complexes) and allow **1-H** and **2-H** to sample these asymmetric reactive structures (i.e., terminal or asymmetrically bridging hydrides). However, the two unreacted hydrides in complexes **1-CO$_2$** and **2-CO$_2$** are unable to access terminal or asymmetric bridging modes because the steric demand imposed by the formate adds to the overall thermodynamic cost for hydride transfer. We observed that the formate ligand in the trizinc

DOI: 10.1021/jacs.5b05204
J. Am. Chem. Soc. 2015, 137, 10610−10617

analog of **1-CO$_2$** is fluxional in solution on the NMR time scale with activation parameters consistent with a carboxylate shift.[14] We anticipate that the formate in **1-CO$_2$** and **2-CO$_2$** is similarly fluxional. The weaker M−H bonds in **1-CO$_2$** as compared to **2-CO$_2$** allow for thermal activation of the remaining two hydrides to afford **1-3CO$_2$**, whereas the analogous tricobalt complex is not observed under similar conditions. In this mechanism, reactivity is controlled by a combination of the electronic effects and the structural constraints imposed by the ligand. The CV data support the combined control of the reactivity of **1-CO$_2$** and **2-CO$_2$** proposed in mechanism B. However, we cannot exclude reactions (e.g., formate loss, hydride abstraction from solvent) in the electrochemical cell at the strongly reducing potentials.

We were surprised that neither **1-** nor **2-H** reductively eliminates dihydrogen, which contrasts with the monoiron analog and the current mechanism proposed for the E$_4$ state of FeMoco. Our finding supports recent work by Peters and co-workers in which N$_2$ binding is faster after reduction of hydride-bridged diiron compounds, suggesting that H$_2$ elimination may not be essential for substrate coordination to nitrogenase.[25b,36] Minor changes to cluster nuclearity and structure evidently tune the stability of the (β-diketiminato)iron hydride fragments, suggesting that similar effects can be present in FeMoco.

CONCLUSION

Planar trinuclear iron(II) or cobalt(II) tri(hydride) clusters were synthesized using a cyclophane ligand to template cluster assembly. These metal hydrides react selectively with CO$_2$ to generate a monoformate di(hydride) trimetallic species as the first isolable product. All hydrides in the triiron complex, **1-H**, react at elevated temperatures, whereas no further reaction is observed beyond formation of **2-CO$_2$** with the tricobalt complex. Isolation of formate adducts from **1-CO$_2$** or **2-CO$_2$** and regeneration of the starting materials to construct catalytic cycles are in progress, as are the synthesis and reactivity studies of complexes containing coordinatively unsaturated hydride-bridged clusters.

ASSOCIATED CONTENT

Supporting Information

The Supporting Information is available free of charge on the ACS Publications website at DOI: 10.1021/jacs.5b05204.

Supporting figures and tables (Figures S1−S14 and Tables S2−S9) (PDF)
X-ray crystallographic data for **2** (CIF)
X-ray crystallographic data for **2-H** (CIF)
X-ray crystallographic data for **2-CO$_2$** (CIF)
X-ray crystallographic data for **1-3CO$_2$** (CIF)
X-ray crystallographic data for **1-H** (CIF)
X-ray crystallographic data for **1-CO$_2$** (CIF)

AUTHOR INFORMATION

Corresponding Author

*murray@chem.ufl.edu

Notes

The authors declare no competing financial interests.

ACKNOWLEDGMENTS

L.J.M. acknowledges the University of Florida, the ACS Petroleum Research Fund (ACS-PRF 52704-DNI3), and the National Science Foundation (CHE-1464876) for support and a departmental instrumentation award from the National Science Foundation (CHE-1048604). K.A.A. acknowledges the National Science Foundation (CHE-0821346) and the University of Florida for funding of the purchase of the X-ray equipment. R.G.S. acknowledges the support of Labex ARCANE (ANR-11-LABX-0003-01). We thank Dr. Geneviève Blondin for helpful discussions.

REFERENCES

(1) (a) Benson, E. E.; Kubiak, C. P.; Sathrum, A. J.; Smieja, J. M. *Chem. Soc. Rev.* **2009**, *38*, 89. (b) Centi, G.; Quadrelli, E. A.; Perathoner, S. *Energy Environ. Sci.* **2013**, *6*, 1711. (c) Quadrelli, E. A.; Centi, G.; Duplan, J.-L.; Perathoner, S. *ChemSusChem* **2011**, *4*, 1194. (d) Enthaler, S.; von Langermann, J.; Schmidt, T. *Energy Environ. Sci.* **2010**, *3*, 1207.

(2) (a) Yin, X.; Moss, J. R. *Coord. Chem. Rev.* **1999**, *181*, 27. (b) Appel, A. M.; Bercaw, J. E.; Bocarsly, A. B.; Dobbek, H.; DuBois, D. L.; Dupuis, M.; Ferry, J. G.; Fujita, E.; Hille, R.; Kenis, P. J. A.; Kerfeld, C. A.; Morris, R. H.; Peden, C. H. F.; Portis, A. R.; Ragsdale, S. W.; Rauchfuss, T. B.; Reek, J. N. H.; Seefeldt, L. C.; Thauer, R. K.; Waldrop, G. L. *Chem. Rev.* **2013**, *113*, 6621. (c) Wang, W.; Wang, S.; Ma, X.; Gong, J. *Chem. Soc. Rev.* **2011**, *40*, 3703. (d) Jessop, P. G.; Ikariya, T.; Noyori, R. *Chem. Rev.* **1995**, *95*, 259. (e) Jessop, P. G.; Joó, F.; Tai, C.-C. *Coord. Chem. Rev.* **2004**, *248*, 2425.

(3) DuBois, D. L.; Berning, D. E. *Appl. Organomet. Chem.* **2000**, *14*, 860.

(4) (a) Jeletic, M. S.; Mock, M. T.; Appel, A. M.; Linehan, J. C. *J. Am. Chem. Soc.* **2013**, *135*, 11533. (b) Qi, X.-J.; Liu, L.; Fu, Y.; Guo, Q.-X. *Organometallics* **2006**, *25*, 5879. (c) Qi, X.-J.; Fu, Y.; Liu, L.; Guo, Q.-X. *Organometallics* **2007**, *26*, 4197.

(5) (a) Berning, D. E.; Noll, B. C.; DuBois, D. L. *J. Am. Chem. Soc.* **1999**, *121*, 11432. (b) Sarker, N.; Bruno, J. W. *J. Am. Chem. Soc.* **1999**, *121*, 2174.

(6) (a) Cheng, T.-Y.; Brunschwig, B. S.; Bullock, R. M. *J. Am. Chem. Soc.* **1998**, *120*, 13121. (b) Franz, J. A.; Kolwaite, D. S.; Linehan, J. C.; Rosenberg, E. *Organometallics* **2004**, *23*, 441.

(7) (a) Yu, Y.; Sadique, A. R.; Smith, J. M.; Dugan, T. R.; Cowley, R. E.; Brennessel, W. W.; Flaschenriem, C. J.; Bill, E.; Cundari, T. R.; Holland, P. L. *J. Am. Chem. Soc.* **2008**, *130*, 6624. (b) Dugan, T. R.; Bill, E.; MacLeod, K. C.; Brennessel, W. W.; Holland, P. L. *Inorg. Chem.* **2014**, *53*, 2370. (c) Yu, Y.; Brennessel, W. W.; Holland, P. L. *Organometallics* **2007**, *26*, 3217. (d) Smith, J. M.; Sadique, A. R.; Cundari, T. R.; Rodgers, K. R.; Lukat-Rodgers, G.; Lachicotte, R. J.; Flaschenriem, C. J.; Vela, J.; Holland, P. L. *J. Am. Chem. Soc.* **2006**, *128*, 756.

(8) Barton, B. E.; Rauchfuss, T. B. *Inorg. Chem.* **2008**, *47*, 2261.

(9) Wang, W.; Nilges, M. J.; Rauchfuss, T. B.; Stein, M. *J. Am. Chem. Soc.* **2013**, *135*, 3633.

(10) (a) Hoffman, B. M.; Lukoyanov, D.; Yang, Z.-Y.; Dean, D. R.; Seefeldt, L. C. *Chem. Rev.* **2014**, *114*, 4041. (b) Hoffman, B. M.; Lukoyanov, D.; Dean, D. R.; Seefeldt, L. C. *Acc. Chem. Res.* **2013**, *46*, 587. (c) Lukoyanov, D.; Yang, Z.-Y.; Dean, D. R.; Seefeldt, L. C.; Hoffman, B. M. *J. Am. Chem. Soc.* **2010**, *132*, 2526. (d) Doan, P. E.; Telser, J.; Barney, B. M.; Igarashi, R. Y.; Dean, D. R.; Seefeldt, L. C.; Hoffman, B. M. *J. Am. Chem. Soc.* **2011**, *133*, 17329. (e) Dance, I. *Chem. Commun.* **2013**, *49*, 10893. (f) Dance, I. *J. Am. Chem. Soc.* **2005**, *127*, 10925.

(11) Igarashi, R. Y.; Laryukhin, M.; Dos Santos, P. C.; Lee, H.-I.; Dean, D. R.; Seefeldt, L. C.; Hoffman, B. M. *J. Am. Chem. Soc.* **2005**, *127*, 6231.

(12) (a) Fantucci, P. *J. Organomet. Chem.* **1976**, *108*, 203. (b) Kaesz, H. D.; Knox, S. A. R. *J. Am. Chem. Soc.* **1971**, *93*, 4594. (c) Barton, B. E.; Zampella, G.; Justice, A. K.; De Gioia, L.; Rauchfuss, T. B.; Wilson, S. R. *Dalton Trans.* **2010**, *39*, 3011. (d) Nevinger, L. R.; Keister, J. B. *Organometallics* **1990**, *9*, 2312. (e) Day, V. W.; Fredrich, M. F.; Reddy, G. S.; Sivak, A. J.; Pretzer, W. R.; Muetterties, E. L. *J. Am. Chem. Soc.* **1977**, *99*, 8091. (f) Powell, J.; Gregg, M. R.; Sawyer, J. F. *J. Chem. Soc., Chem. Commun.* **1987**, 1029. (g) Eady, C. R.; Johnson, B. F. G.; Lewis,

DOI: 10.1021/jacs.5b05204
J. Am. Chem. Soc. 2015, 137, 10610−10617

J. *J. Chem. Soc., Chem. Commun.* **1976**, 302. (h) Koepke, J. W.; Johnson, J. R.; Knox, S. A. R.; Kaesz, H. D. *J. Am. Chem. Soc.* **1975**, *97*, 3947. (i) Shapley, J. R.; Richter, S. I.; Churchill, M. R.; Lashewycz, R. A. *J. Am. Chem. Soc.* **1977**, *99*, 7384. (j) Keister, J. B.; Frey, U.; Zbinden, D.; Merbach, A. E. *Organometallics* **1991**, *10*, 1497. (k) Wilson, R. D.; Bau, R. *J. Am. Chem. Soc.* **1976**, *98*, 4687.

(13) (a) Dugan, T. R.; Goldberg, J. M.; Brennessel, W. W.; Holland, P. L. *Organometallics* **2012**, *31*, 1349. (b) Ding, K.; Brennessel, W. W.; Holland, P. L. *J. Am. Chem. Soc.* **2009**, *131*, 10804. (c) Pfirrmann, S.; Limberg, C.; Ziemer, B. *Dalton Trans.* **2008**, 6689. (d) Pfirrmann, S.; Limberg, C.; Herwig, C.; Knispel, C.; Braun, B.; Bill, E.; Stösser, R. *J. Am. Chem. Soc.* **2010**, *132*, 13684. (e) Dong, Q.; Zhao, Y.; Su, Y.; Su, J.-H.; Wu, B.; Yang, X.-J. *Inorg. Chem.* **2012**, *51*, 13162.

(14) Ermert, D. M.; Ghiviriga, I.; Catalano, V. J.; Shearer, J.; Murray, L. J. *Angew. Chem., Int. Ed.* **2015**, *54*, 7047.

(15) (a) Smith, J. M.; Lachicotte, R. J.; Holland, P. L. *J. Am. Chem. Soc.* **2003**, *125*, 15752. (b) Bendt, G.; Schulz, S.; Spielmann, J.; Schmidt, S.; Bläser, D.; Wölper, C. *Eur. J. Inorg. Chem.* **2012**, 3725. (c) Boone, C.; Korobkov, I.; Nikonov, G. I. *ACS Catal.* **2013**, *3*, 2336.

(16) (a) Evans, D. F. *J. Chem. Soc.* **1959**, 2003. (b) Bain, G. A.; Berry, J. F. *J. Chem. Educ.* **2008**, *85*, 532. (c) Sur, S. K. *J. Magn. Reson.* **1989**, *82*, 169. (d) Schubert, E. M. *J. Chem. Educ.* **1992**, *69*, 62.

(17) Fryzuk, M. D.; Lloyd, B. R.; Clentsmith, G. K. B.; Rettig, S. J. *J. Am. Chem. Soc.* **1994**, *116*, 3804.

(18) Guillet, G. L.; Sloane, F. T.; Ermert, D. M.; Calkins, M. W.; Peprah, M. K.; Knowles, E. S.; Čižmár, E.; Abboud, K. A.; Meisel, M. W.; Murray, L. J. *Chem. Commun.* **2013**, *49*, 6635.

(19) Bailey, P. J.; Coxall, R. A.; Dick, C. M.; Fabre, S.; Henderson, L. C.; Herber, C.; Liddle, S. T.; Loroño-González, D.; Parkin, A.; Parsons, S. *Chem. - Eur. J.* **2003**, *9*, 4820.

(20) Yang, L.; Powell, D. R.; Houser, R. P. *Dalton Trans.* **2007**, 955.

(21) (a) Di Francesco, G. N.; Gaillard, A.; Ghiviriga, I.; Abboud, K. A.; Murray, L. J. *Inorg. Chem.* **2014**, *53*, 4647. (b) Murray, L. J.; Weare, W. W.; Shearer, J.; Mitchell, A. D.; Abboud, K. A. *J. Am. Chem. Soc.* **2014**, *136*, 13502.

(22) Holland, P. L.; Cundari, T. R.; Perez, L. L.; Eckert, N. A.; Lachicotte, R. J. *J. Am. Chem. Soc.* **2002**, *124*, 14416.

(23) Vela, J.; Smith, J. M.; Yu, Y.; Ketterer, N. A.; Flaschenriem, C. J.; Lachicotte, R. J.; Holland, P. L. *J. Am. Chem. Soc.* **2005**, *127*, 7857.

(24) Rodriguez, M. M.; Bill, E.; Brennessel, W. W.; Holland, P. L. *Science* **2011**, *334*, 780.

(25) Jablonskytė, A.; Wright, J. A.; Fairhurst, S. A.; Webster, L. R.; Pickett, C. J. *Angew. Chem., Int. Ed.* **2014**, *53*, 10143. (b) Rittle, J.; McCrory, C. C. L.; Peters, J. C. *J. Am. Chem. Soc.* **2014**, *136*, 13853. (c) Brown, S. D.; Mehn, M. P.; Peters, J. C. *J. Am. Chem. Soc.* **2005**, *127*, 13146. (d) Kersten, J. L.; Rheingold, A. L.; Theopold, K. H.; Casey, C. P.; Widenhoefer, R. A.; Hop, C. E. C. A. *Angew. Chem., Int. Ed. Engl.* **1992**, *31*, 1341. (e) Nishihara, Y.; Deck, K. J.; Shang, M.; Fehlner, T. P. *J. Am. Chem. Soc.* **1993**, *115*, 12224. (f) Dapporto, P.; Midollini, S.; Sacconi, L. *Inorg. Chem.* **1975**, *14*, 1643. (g) Bortz, M.; Bau, R.; Schneider, J. J.; Mason, S. A. *J. Cluster Sci.* **2001**, *12*, 285. (h) Hanson, B. E.; Fanwick, P. E.; Mancinila, J. S. *Inorg. Chem.* **1982**, *21*, 3811.

(26) Lee, Y.; Sloane, F. T.; Blondin, G.; Abboud, K. A.; García-Serres, R.; Murray, L. J. *Angew. Chem., Int. Ed.* **2015**, *54*, 1499.

(27) (a) Cowley, R. E.; Holland, P. L. *Inorg. Chem.* **2012**, *51*, 8352. (b) Dugan, T. R.; Sun, X.; Rybak-Akimova, E. V.; Olatunji-Ojo, O.; Cundari, T. R.; Holland, P. L. *J. Am. Chem. Soc.* **2011**, *133*, 12418.

(28) (a) Tolman, W. B.; Liu, S.; Bentsen, J. G.; Lippard, S. J. *J. Am. Chem. Soc.* **1991**, *113*, 152. (b) Tolman, W. B.; Bino, A.; Lippard, S. J. *J. Am. Chem. Soc.* **1989**, *111*, 8522.

(29) (a) Wang, J.; Luo, J.; Zhao, J.; Li, D.-S.; Li, G.; Huo, Q.; Liu, Y. *Cryst. Growth Des.* **2014**, *14*, 2375. (b) Zhao, J.-P.; Han, S.-D.; Zhao, R.; Yang, Q.; Chang, Z.; Bu, X.-H. *Inorg. Chem.* **2013**, *52*, 2862.

(30) (a) Beinert, H.; Holm, R. H.; Münck, E. *Science* **1997**, *277*, 653. (b) Albers, A.; Demeshko, S.; Pröpper, K.; Dechert, S.; Bill, E.; Meyer, F. *J. Am. Chem. Soc.* **2013**, *135*, 1704. (c) Dugan, T. R.; Holland, P. L. *J. Organomet. Chem.* **2009**, *694*, 2825.

(31) Ermert, D. M.; Anderton, K. J.; Quintero, P. A.; Turvey, M. W.; Abboud, K. A.; Meisel, M. W.; Murray, L. J. Manuscript in preparation.

(32) DuBois, D. L.; Blake, D. M.; Miedaner, A.; Curtis, C. J.; DuBois, M. R.; Franz, J. A.; Linehan, J. C. *Organometallics* **2006**, *25*, 4414.

(33) Fong, H.; Peters, J. C. *Inorg. Chem.* **2015**, *54*, 5124.

(34) (a) Seefeldt, L. C.; Yang, Z.-Y.; Duval, S.; Dean, D. R. *Biochim. Biophys. Acta, Bioenerg.* **2013**, *1827*, 1102. (b) Yang, Z.-Y.; Moure, V. R.; Dean, D. R.; Seefeldt, L. C. *Proc. Natl. Acad. Sci. U. S. A.* **2012**, *109*, 19644.

(35) (a) Bontemps, S.; Vendier, L.; Sabo-Etienne, S. *Angew. Chem., Int. Ed.* **2012**, *51*, 1671. (b) Huff, C. A.; Sanford, M. S. *ACS Catal.* **2013**, *3*, 2412. (c) Langer, R.; Diskin-Posner, Y.; Leitus, G.; Shimon, L. J. W.; Ben-David, Y.; Milstein, D. *Angew. Chem., Int. Ed.* **2011**, *50*, 9948. (d) Schmeier, T. J.; Dobereiner, G. E.; Crabtree, R. H.; Hazari, N. *J. Am. Chem. Soc.* **2011**, *133*, 9274. (e) Davies, C. J. E.; Lowe, J. P.; Mahon, M. F.; Poulten, R. C.; Whittlesey, M. K. *Organometallics* **2013**, *32*, 4927. (f) Namura, K.; Ohashi, M.; Suzuki, H. *Organometallics* **2012**, *31*, 5979. (g) Namura, K.; Suzuki, H. *Organometallics* **2014**, *33*, 2968. (h) Lyons, D.; Wilkinson, G.; Thornton-Pett, M.; Hursthouse, M. B. *J. Chem. Soc., Dalton Trans.* **1984**, 695.

(36) Creutz, S. E.; Peters, J. C. *J. Am. Chem. Soc.* **2015**, *137*, 7310.

NOTE ADDED AFTER ASAP PUBLICATION

With approval of the Editor, the fourth author listed was added after the paper was published ASAP on August 13, 2015. The revised version was reposted on August 17, 2015.

DOI: 10.1021/jacs.5b05204
J. Am. Chem. Soc. 2015, 137, 10610−10617